Robust Return Algorithm for Anisotropic Plasticity Models

Tidemann, L.; Krenk, Steen

Published in:
Proceedings of the 30th Nordic Seminar on Computational Mechanics (NSCM-30)

Publication date:
2017

Document Version
Publisher's PDF, also known as Version of record

30th Nordic Seminar on Computational Mechanics
NSCM-30
J. Høgsberg. N.L. Pedersen (Eds.)
2017

ROBUST RETURN ALGORITHM FOR ANISOTROPIC PLASTICITY MODELS

L. TIDEMANN*† AND S. KRENK*

*Department of Mechanical Engineering, Technical University of Denmark
DK-2800 Kongens Lyngby, Denmark

†Mærsk Olie & Gas
DK-6700 Esbjerg, Denmark
e-mail: lastid@mek.dtu.dk

Key words: Return algorithms, Computational methods, Cyclic plasticity.

1 INTRODUCTION

Plasticity models can be defined by an energy potential, a plastic flow potential and a yield surface. The energy potential defines the relation between the observable elastic strains $\boldsymbol{\gamma}_\mathrm{e}$ and the energy conjugate stresses $\boldsymbol{\tau}_\mathrm{e}$ and between the non-observable internal strains $\boldsymbol{\gamma}_\mathrm{i}$ and the energy conjugate internal stresses $\boldsymbol{\tau}_\mathrm{i}$, where the internal stresses control the various hardening mechanisms. Plasticity models may be defined either in terms of traditional stresses and strains $\boldsymbol{\tau} = [\sigma_{11}, \sigma_{22}, \cdots]^T$ and $\boldsymbol{\gamma} = [\varepsilon_{11}, \varepsilon_{22}, \cdots]^T$ or generalized stresses and strains, e.g. $\boldsymbol{\tau} = [N, M_y, \cdots]^T$ and $\boldsymbol{\gamma} = [\varepsilon, \kappa_y, \cdots]^T$, the latter typically used in plastic analysis of frame structures. To have a compact notation in the following $\boldsymbol{\tau}_\mathrm{e}$ and $\boldsymbol{\tau}_\mathrm{i}$ are arranged in a common vector $\tilde{\boldsymbol{\tau}}^T = [\boldsymbol{\tau}_\mathrm{e}^T, \boldsymbol{\tau}_\mathrm{i}^T]$ and correspondingly $\boldsymbol{\gamma}_\mathrm{e}$ and $\boldsymbol{\gamma}_\mathrm{i}$ are arranged in the common vector $\tilde{\boldsymbol{\gamma}}^T = [\boldsymbol{\gamma}_\mathrm{e}^T, \boldsymbol{\gamma}_\mathrm{i}^T]$.

In traditional stress-based analyses the stress is evaluated at a material point, where a single plastic mechanism may be active, whereas in the case of frame structures each beam may have two active plastic mechanisms, in the form of a yield hinge in each end as illustrated in Fig. 1. In general multiple plastic mechanisms may be active for different types of elements. Each plastic mechanism has a yield surface described by a yield function F_j and a flow potential G_j describing the plastic flow evolution by its gradient and these potentials are conveniently collected in the vectors $\mathbf{f}_y = [F_1(\tilde{\boldsymbol{\tau}}), \dots, F_n(\tilde{\boldsymbol{\tau}})]^T$ and $\mathbf{g} = [G_1(\tilde{\boldsymbol{\tau}}), \dots, G_n(\tilde{\boldsymbol{\tau}})]^T$ respectively.

The key to developing a general and robust return algorithm for anisotropic plasticity models is the strain evolution equation. The strain evolution equation is obtained from maximizing the dissipation rate under the assumption that the material is described by the flow potential[1,2]

$$\dot{\tilde{\boldsymbol{\gamma}}} = \begin{bmatrix} \dot{\boldsymbol{\gamma}}_\mathrm{t} \\ \mathbf{0} \end{bmatrix} - \sum_j \partial_{\tilde{\boldsymbol{\tau}}} G_j \, \dot{\lambda}_j = \begin{bmatrix} \dot{\boldsymbol{\gamma}}_\mathrm{t} \\ \mathbf{0} \end{bmatrix} - \left(\partial_{\tilde{\boldsymbol{\tau}}}^T \mathbf{g}\right)^T \dot{\boldsymbol{\lambda}} \,, \tag{1}$$

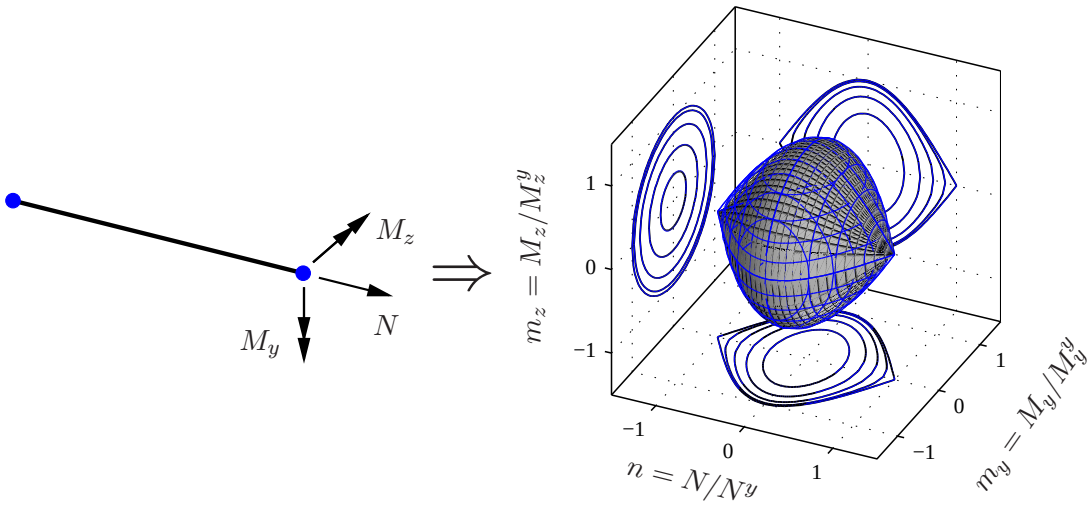

Figure 1: Beam with plastic hinges and corresponding yield surface.

where $\dot{\boldsymbol{\gamma}}_{\mathrm{t}}$ is the total increment in the observable strains. The plastic multipliers $\dot{\boldsymbol{\lambda}}$ are determined by the consistency condition that during plastic loading, the stress state $\boldsymbol{\tau}_{\mathrm{e}}$ must stay on the yield surfaces defined in $\mathbf{f}_y$.

2 RETURN ALGORITHM

The strain evolution equation (1) is reformulated to finite increments and is assumed to be satisfied in the final generalized stress state[3]. For non-trivial yield surfaces the strain evolution equation will not initially be satisfied and a residual is formed

$$\mathbf{r}_{\tilde{\gamma}} \;=\; \begin{bmatrix} \Delta\boldsymbol{\gamma}_{\mathrm{t}} \\ \mathbf{0} \end{bmatrix} - \Delta\tilde{\boldsymbol{\gamma}} - \left(\partial_{\tilde{\boldsymbol{\tau}}}^T \mathbf{g}\right)^T \Delta\boldsymbol{\lambda}\,. \tag{2}$$

The final state where $\mathbf{r}_{\tilde{\gamma}} = \mathbf{0}$ is obtained by a first order variation of the residual (2) combined with the consistency condition that the final stress state must be on the yield surface. The first order variation is formulated entirely in terms of $\delta\tilde{\boldsymbol{\tau}}$ and $\delta\boldsymbol{\lambda}$ with use of the constitutive relation

$$\delta\tilde{\boldsymbol{\tau}} \;=\; \tilde{\mathbf{K}}\,\delta\tilde{\boldsymbol{\gamma}}\,, \tag{3}$$

where the tangent stiffness matrix $\tilde{\mathbf{K}}$ contains the double derivatives of the energy potential. The resulting equation system to solve is

$$\begin{bmatrix} \tilde{\mathbf{K}}_A^{-1} & \left(\partial_{\tilde{\boldsymbol{\tau}}}^T \mathbf{g}\right)^T \\ \partial_{\tilde{\boldsymbol{\tau}}}^T \mathbf{f}_y & \mathbf{0} \end{bmatrix} \begin{bmatrix} \delta\tilde{\boldsymbol{\tau}} \\ \delta\boldsymbol{\lambda} \end{bmatrix} \;=\; \begin{bmatrix} \mathbf{r}_{\tilde{\gamma}} \\ -\mathbf{f}_y \end{bmatrix}\,, \quad \tilde{\mathbf{K}}_A^{-1} \;=\; \tilde{\mathbf{K}}^{-1} + \sum_j \frac{\partial^2 G_j}{\partial\tilde{\boldsymbol{\tau}}^T \partial\tilde{\boldsymbol{\tau}}} \Delta\lambda_j\,, \tag{4}$$

where $\tilde{\mathbf{K}}_A$ is the consistent algorithmic stiffness matrix. Instead of solving (4) directly it is solved sequentially by eliminating $\delta\tilde{\boldsymbol{\tau}}$ in the first equation and determining $\delta\boldsymbol{\lambda}$ from the second equation and back-substituting the result into the first equation. Anisotropic

plasticity models may have yield surfaces with regions with large curvature, Fig. 1, leading to large changes in the direction of the gradient of the yield surface and the plastic flow potential. Though $\delta\tilde{\boldsymbol{\tau}}$ is a linear function of the residual $\mathbf{r}_{\tilde{\gamma}}$ and the value of the yield function $\mathbf{f}_y$ according to (4) the function is non-linear as $\tilde{\mathbf{K}}_A^{-1}$, $\partial_{\tilde{\boldsymbol{\tau}}}^T\mathbf{g}$ and $\partial_{\tilde{\boldsymbol{\tau}}}^T\mathbf{f}_y$ in general are non-linear. The increment $\delta\tilde{\boldsymbol{\tau}} = \delta\tilde{\boldsymbol{\tau}}(\xi\mathbf{r}_{\tilde{\gamma}}, \xi\mathbf{f}_y)$ is therefore represented by a second order approximation

$$\delta\tilde{\boldsymbol{\tau}}(\xi) \;=\; \xi\,\frac{\partial(\delta\tilde{\boldsymbol{\tau}})}{\partial\xi}\bigg|_{\xi=0} + \tfrac{1}{2}\xi^2\frac{\partial^2(\delta\tilde{\boldsymbol{\tau}})}{\partial\xi^2}\bigg|_{\xi=0}, \tag{5}$$

where the constant term is zero for $\xi = 0$ and the two derivatives are given by

$$\frac{\partial(\delta\tilde{\boldsymbol{\tau}})}{\partial\xi} \;=\; \mathbf{K}_\mathbf{r}\mathbf{r}_{\tilde{\gamma}} - \mathbf{K}_\mathbf{f}\mathbf{f}_y\,, \quad \frac{\partial^2(\delta\tilde{\boldsymbol{\tau}})}{\partial^2\xi} \;=\; \frac{\partial}{\partial\xi}\Big(\mathbf{K}_\mathbf{r}\mathbf{r}_{\tilde{\gamma}} - \mathbf{K}_\mathbf{f}\mathbf{f}_y\Big) \;\simeq\; \frac{\Delta\mathbf{K}_\mathbf{r}}{\Delta\xi}\mathbf{r}_{\tilde{\gamma}} - \frac{\Delta\mathbf{K}_\mathbf{f}}{\Delta\xi}\mathbf{f}_y\,. \tag{6}$$

The differences $\Delta\mathbf{K}_\mathbf{r}$ and $\Delta\mathbf{K}_\mathbf{f}$ are determined by making half a step, i.e. setting $\xi = 1/2$ and determining the matrices in the updated state by the gradients $\partial_{\tilde{\boldsymbol{\tau}}}^T\mathbf{g}$ and $\partial_{\tilde{\boldsymbol{\tau}}}^T\mathbf{f}_y$ as well as the second order derivatives $\partial^2 G_j/(\partial\tilde{\boldsymbol{\tau}}^T\partial\tilde{\boldsymbol{\tau}})$. These are combined with the solution of the equation system (4) to form $\mathbf{K}_\mathbf{r}^{1/2}$ and $\mathbf{K}_\mathbf{f}^{1/2}$. Inserting the results into (6) and (5) with $\Delta\xi = 1/2$ and setting $\xi = 1$ gives the relation

$$\delta\tilde{\boldsymbol{\tau}} \;=\; \mathbf{K}_\mathbf{r}^{1/2}\mathbf{r}_{\tilde{\gamma}} - \mathbf{K}_\mathbf{f}^{1/2}\mathbf{f}_y\,. \tag{7}$$

This is analogous to a method used in explicit stress integration[3] where a midpoint is found and the elasto-plastic stiffness at the midpoint is used for a full step.

3 NUMERICAL EXAMPLES

The robustness of the return algorithm is illustrated by deformation of a beam with plastic hinges, Fig. 1, described by a cyclic plasticity model[1] in terms of the normalized section forces[2] $n = N/M^y$ and $m = M/M^y$. The yield surface is slightly rounded in comparison to the one shown in Fig. 1. The energy potential consists of two quadratic terms uncoupling $\boldsymbol{\tau}_\mathrm{e}$ and $\boldsymbol{\tau}_\mathrm{i}$ whereby $\tilde{\mathbf{K}}$ becomes a block diagonal matrix with $\mathbf{K}_\mathrm{e}$ and $\mathbf{K}_\mathrm{i}$ in the diagonals. The yield surface is kinematic hardening and is tailored for cyclic plasticity models with general hardening behaviour[1]. The beam is modelled with parameters representing ideal-plastic behaviour, Fig. 2(a) and (b), and parameters representing non-linear hardening plastic hinges, Fig. 2(c) and (d). Both beams are subjected to a large strain increment with an equivalent estimated elastic stress state with $n = 14$ and $m_y = 4$ at one hinge and $n = 14$ and $m_y = 0$ at the other hinge.

The estimated elastic stress state is located far away from the yield surface in a region with relatively large curvature of the yield surface and two plastic mechanisms. Nevertheless the algorithm returns the stress state to the yield surfaces in just 10 iterations in the ideal plasticity case as illustrated in Fig. 2(a) and (b). About half the number of iterations is used to get to the neighbourhood of the final state and the remaining half is

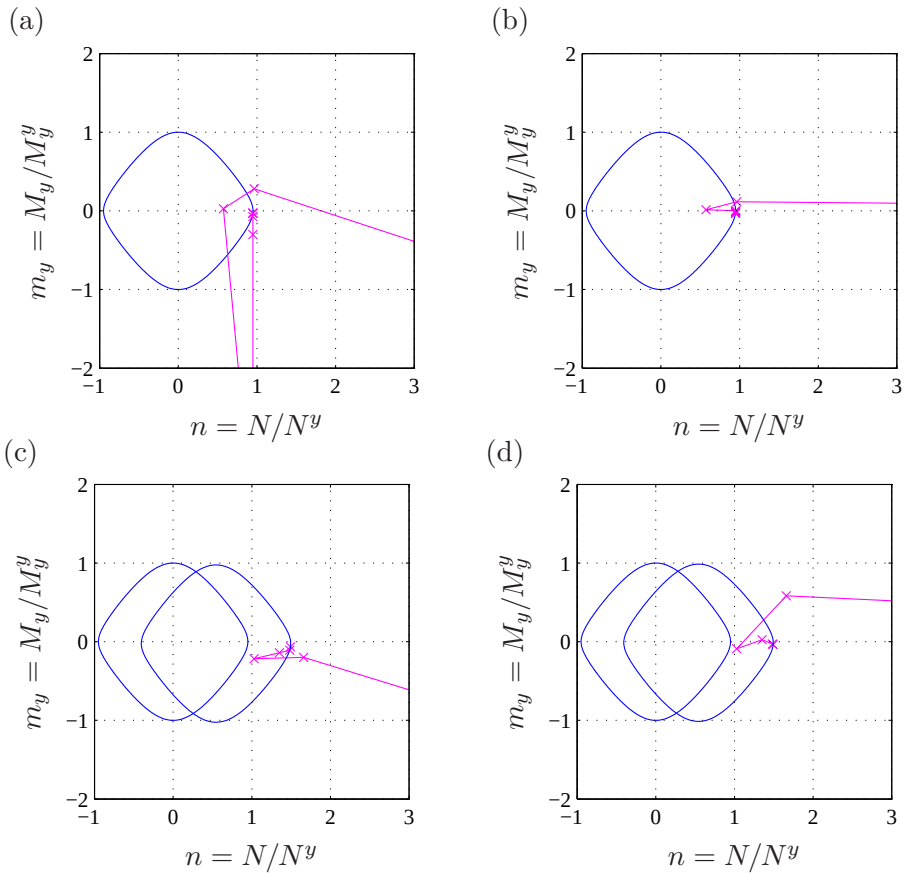

Figure 2: Return with ideal plasticity parameters (top) and hardening plasticity parameters (bottom). Left: Yield surface 1. Right: Yield surface 2.

to ensure $\mathbf{r}_{\tilde{\gamma}} = \mathbf{0}$. Hardening typically eases return and as shown in Fig. 2(c) and (d) it does in the present case as well, as the return is made in only 7 steps. It is noted that a traditional single-step return algorithm fails to converge for the predicted stress states shown in Fig. 2. In general the method presented here is more robust, e.g. if half the deformation increment used above is applied a traditional single-step return algorithm will converge in the ideal-plastic case but not in the hardening case.

REFERENCES

[1] Krenk, S. & Tidemann, L. A compact cyclic plasticity model with parameter evolution. *Mechanics of Materials* **113**, 57–68 (2017).

[2] Tidemann, L. & Krenk, S. Cyclic plastic hinges with degradation effects for frame structures. *Journal of Engineering Mechanics* (accepted for publication) (2017).

[3] Zienkiewicz, O. C., Taylor, R. L. & Zhu, J. Z. *The Finite Element Method* (Elsevier Butterworth–Heinemann, Oxford, 2005), 6 edn.